A Wind Tunnel Study of the Drag Coefficient over Steep Sinusoid Waves

Brian C. Zachry[1,*] and Chris W. Letchford[2]

Introduction

Understanding wind stress over waves near the coast and in the open ocean are paramount to coastal society, with far reaching impacts to forecasting hurricane intensity, storm surge and waves, and prescribing building codes for hurricane prone coastal regions. Since full scale measurements of nearshore drag are a demanding task (and it was not until fairly recently that deep water drag became known), laboratory measurements can offer valuable insight. In this light, a novel laboratory experiment was designed to gather preliminary data to determine the approximate bounds of the drag coefficient utilizing the Boundary Layer Wind Tunnel at Texas Tech University (TTU). Specifically, this work provides knowledge of the drag coefficient C_D over steep (solid) sinusoid and half sinusoid wave shapes via wind profile and pressure measurements. The half sinusoid shape represents an idealized critical (near-breaking) wave, which has two orientations in the wind tunnel in order to simulate offshore and onshore wind flow regimes (Figure 6). This shape provides an upper limit for drag. For simplicity, this study classifies near-breaking by a half sinusoid shape rather than an increase in steepness and no deformation to wave shape. The full sinusoid shape represents an 'ideal' deep water swell type wave with minimum drag (lower bound). Results from this work are compared to other laboratory and observational studies. This study also examines the form drag coefficient (via surface pressure measurements) and the feasibility of stationary waves using a similar experiment conducted in the TTU wind tunnel by Chen (2007).

Methodology

The TTU wind tunnel is of the closed-circuit type and is powered by a 250 hp fan, which is capable of generating wind speeds in excess of 25 m/s in the boundary layer test section (1.8 m wide by 1.2 m high). Over a fetch length of 15.2 m the boundary layer can grow naturally to a nominal thickness of 0.3-0.5 m at a wind speed of 10 m/s. Several augmentation devices were used to simulate the atmospheric boundary layer, including a plane of honeycomb material, two fine mesh screens, four equally spaced spires (1140 mm high), and a fence barrier (235 mm tall). A relatively smooth simulation was conducted for this study by placing carpet along the wind tunnel fetch length, which generates a profile similar to Exposures C.

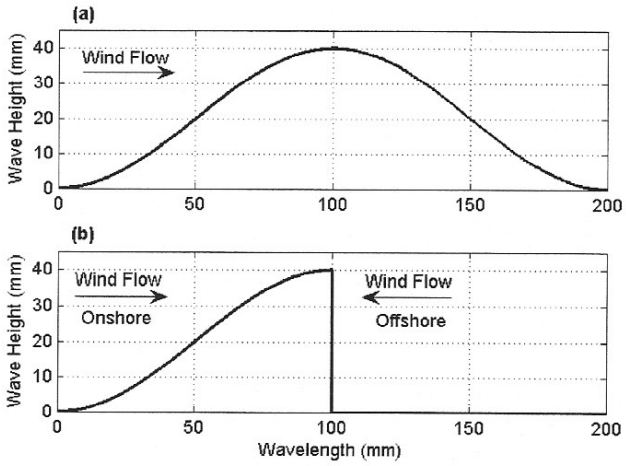

Figure 6: Model scale wave profiles: (a) full sinusoid deep water wave and (b) half sinusoid near-breaking wave in onshore and offshore wind regimes

Sinusoid and half sinusoid wave shapes were precisely constructed using a 3-D plastic printer. Wave surface elevations are described by $z_s = A\cos(kx)$, where A is the wave amplitude, λ is the wavelength, $k = 2\pi/\lambda$ is the wavenumber, and x is the horizontal coordinate. Four replicas of each wave were printed with wavelength $\lambda = 200$ mm, trough to crest wave height $H = 2A = 40$ mm, width $W = 250$ mm, and thickness $\delta = 3$ mm (Figure 6). A common measure of a wave profile is the wave height to wavelength aspect ratio H/λ. Typical values for steep laboratory waves are on the order of 0.2 (e.g., Kawamura and Toba 1988; Csanday 2001), here $40/200 = 0.2$. The full sinusoid wave will be referred to as wave type one (WT1) and the half sinusoid onshore and offshore orientations as WT2 and WT3,

[1] Wind Science and Engineering Research Center, Texas Tech University, Lubbock, TX, USA 79409.
[*] Corresponding author, Email: brian.c.zachry@ttu.edu
[2] School of Engineering, University of Tasmania, Hobart, Tasmania, Australia 7001

respectively. The onshore wind flow regime results when the vertical bluff faces leeward and the offshore condition when the bluff faces windward (Figure 6).

The length scales selected for this experiment are given in Table 4. Length and velocity scales were chosen to simulate wave heights generated in wind speeds ranging from moderate to hurricane force. The reference wind speeds U_{10} in Table 4 are the range of full scale wind speeds (including all wave types) after the appropriate velocity scale has been applied. It should be noted that due to the varying length scales of simulation, exact 10 m full scale wind speed measurements were not always obtained. Hence, reference wind speeds were determined as the measurement height nearest to 10 m obtained from the wind tunnel measurements (deviations < 0.5 m), as opposed to using the log-law: differences in U_{10} will be negligible. Model scale heights were scaled to the standard meteorological reference height z_r = 10 m above the displacement plane (height). Using the method demonstrated by Cook (1978), the displacement coefficient was determined to be α = 0.76. With wave heights h_r = 40 mm, the displacement height is d = 30.4 mm. Thus, at the displacement height d = 30.4 mm, the measured height z = 0 mm.

Table 4: Range of length and velocity scales of simulation, corresponding full scale wave heights (m), and the range of 10 m reference height wind speeds (m/s) selected for this experiment.

			Full Scale	
Scale Identifier	**Length Scale**	**Velocity Scale**	**Wave Height (m)**	**U_{10} (m/s)**
A	1:50	1:1	2	12 - 13
B	1:100	1:1.5	4	16 - 19
C	1:150	1:2	6	18 - 23
D	1:200	1:3	8	24 - 33
E	1:250	1:4	10	31 - 44

Each of the four model wave shapes were placed along the centerline of the wind tunnel, oriented perpendicular to the flow, to form a wave train with each successive wave behind the other. Dummy wave models were placed on either side of the precise models in order to facilitate 2-D, periodic flow. Gong et al (1999) found that air flow reaches an almost periodic state by the third or fourth waves. Results from this experiment are analyzed with two waves in front and one behind, allowing the third wave to offer generalized results. A three component Turbulent Flow International Cobra Probe sampling at 1000 Hz attached to an automated traverse measured mean and fluctuating wind velocity component profiles (software package also computes mean profiles for turbulence intensity, and Reynolds stress). The sampling period at each step was 47.104 s, corresponding to 40-60 min of prototype data at each level in the profile. In a similar study, Chen (2007) showed that this sampling time and frequency were sufficient to capture all significant fluctuations. Profiles were sampled directly above the crest and the following trough of the third wave. Surface pressure measurements were taken using a Scanivalve system connected to a data acquisition computer scanning at 300 Hz. Pressure taps were nominally spaced in 12.7 mm increments along the arc of the wave, except for on the vertical bluff where four taps were placed along the 40 mm height. Pressure data were recorded for ~90 s (27,043 scans), providing approximately 75-115 min of full scale data.

The profile (least squares) method was used to estimate of C_D. A least squares best fit line was calculated in MATLAB using the 'polyfit' command to estimate the friction velocity u_* (related to the slope) and roughness length z_o (y-intercept). The drag coefficient C_D was then computed from u_* as follows:

$$C_D = \frac{u_*^2}{U_{10}^2}. \tag{1}$$

Here, C_D represents the total drag exerted on the wave surfaces by the air flow. Form (pressure) drag F_D was determined by integrating the horizontal component of the surface pressure coefficient C_p for each wave type. Form drag is primarily a function of the size and shape, hence 'form' of the object, and results from a combination of positive pressure on the upwind face and negative on the leeward. Form drag was estimated using:

$$F_D = \sum_{i=1}^{n} \frac{\delta\lambda_i C_{pi} \cos(\alpha_i)}{\lambda}, \tag{2}$$

where $\delta\lambda_i$ is the spacing between each tap, C_{Pi} is the pressure coefficient at point i, and $\cos(\alpha_i)$ gives the horizontal component (drag). The form drag coefficient C_{DF} can then be computed as follows:

$$C_{DF} = \frac{F_D}{\frac{1}{2}\overline{\rho}_a \overline{U}_{10}^2}, \quad (3)$$

where ρ_a is the average air density in the wind tunnel.

Results and discussion

Total drag was computed from the crest and trough profiles. All log-law wind profiles showed a strong linear relationship with $R^2 > 0.97$ (after deviations in the wind profile from the log-law in the lowest levels were removed). A characteristic total drag over each wave surface was computed by taking an average of the trough and crest values (Table 5). Trough C_D values are slightly larger than those determined over the crest for WT1 and WT3, but are approximately twice those of the crest for WT2. Based on the characteristic total drag estimates, the deep water ocean surface wave produced the least drag while WT3 observed the largest drags (WT2 in between). This result was anticipated simply by experiment design, and provides a relative bracket for over water drag.

Table 5: Characteristic total drag coefficient estimates (average of crest and trough) over the wave surface.

Scale Identifier	Wave Type	Crest $C_D \times 10^3$	Trough $C_D \times 10^3$	$C_D \times 10^3$
A	1	1.82	1.93	1.87
	2	2.66	4.29	3.48
	3	6.72	6.81	6.76
B	1	2.19	2.26	2.22
	2	3.30	5.30	4.30
	3	8.97	9.20	9.08
C	1	2.33	2.62	2.47
	2	3.63	6.45	5.04
	3	11.1	11.3	11.2
D	1	2.45	2.93	2.69
	2	4.28	7.45	5.86
	3	15.3	15.3	15.3
E	1	2.50	3.07	2.78
	2	4.92	8.80	6.86
	3	17.5	17.5	17.5

In order to confirm the validity of these values, drag coefficient estimates are compared to other studies. Recently, Powell et al. (2003), Black et al. (2007), and Jarosz et al. (2007) made deep water, open ocean measurements of air-sea momentum flux in strong winds associated with hurricanes. Donelan et al. (2004) performed laboratory measurements of C_D in simulated extreme winds. Their results indicate that the C_D increases with wind speed for weak to moderate winds, but reaches a limiting value in strong winds: $C_D \sim 0.0025$ at winds of 33 m/s (Powell et al. 2003; Donelan et al. 2004) and $C_D \sim 0.0018$ at 22-23 m/s (Black et al. 2007). It can be seen that drag values for WT1 are comparable to those mentioned above; however, C_D for WT1 are higher for slower wind speeds < 20 m/s and are only slightly higher for hurricane force winds. This is likely a result of the steep sinusoid wave utilized. In hurricane conditions, waves tend to be steeper and white-capping is frequent, which potentially causes the flow to separate and reattach near the following wave crest. This flow behavior is similar to what was observed here. In regards to the half sinusoid shape, Anctil and Donelan (1996) made measurements over shoaling waves and found drag values on the order of 0.003. Thus the steep, near-breaking onshore flow regime wave shape studied here provides hope that more precise wave shapes can be used to estimate C_D in regions where full scale measurements are seemingly impossible in hurricane conditions.

Estimates of C_{DF} for each wave type are shown in Table 6 and results indicate that form drag is sensitive to wave shape. Two outcomes are of interest: (1) relatively similar values of C_{DF} were observed for WT1 and WT3 and (2) C_{DF} for WT2 were much smaller than the other shapes. It was anticipated that WT3 would have similar but higher values of C_{DF} than the `ideal' wave profile, where the upwind bluff of WT3 produces large positive pressure coefficients, causes the flow to separate, and produces large suction pressures on the leeward side. A most curious result was that obtained for WT2. This behavior is illuminated through wave profile design. The shape of WT2 and the relatively close spacing of the waves leads to skimming flow, so there is very little contribution (if any) to form

drag on the windward side. The four taps on the bluff are the only ones that can contribute to drag on the leeward portion, as the remainder have no slope and thus do not contribute to drag. This work shows that accurate estimates of the form drag coefficient may be rather difficult and need further study.

When dealing with flow over waves, direct comparison of C_{DF} to the total 10 m drag coefficient C_D is not appropriate. It has been suggested that addition of these drag components yields the total drag (e.g., Deardorff 1967). This may be appropriate within the wave boundary layer, but above the wave boundary layer (typically crest height) the wave-coherent stress (form drag) vanishes and the 10 m drag coefficient represents the total drag. In a relative sense, it can be deduced that form drag is at least an order of magnitude smaller than total drag.

Table 6: Form drag estimates for each wave type determined from integrating the horizontal component of the surface pressure coefficients. The form drag coefficient C_{DF} was computed using $C_{DF} = F_D/0.5\rho_a U_{10}^2$, where ρ_a is the mean air density and U_{10} is the 10 m full scale reference wind speed.

Wave Type	ρ_a (kg/m^3)	U_{10} (m/s)	F_D	$C_{DF} * 10^3$
1	1.07	12.9	62.9	0.712
2	1.06	12.8	8.81	0.101
3	1.06	12.8	69.1	0.798

Feasibility of stationary waves

A recent study by Chen (2007) was used to evaluate the feasibility of the work presented. Specifically, it must be determined if stationary waves can be compared to propagating waves. Chen (2007) made measurements over generic smooth (flat belt) and rough (belt with square cleats) moving surfaces at TTU. Results from this experiment can be compared to Chen's rough belt experiment under certain assumptions: (1) assuming a hurricane wave celerity of 10 m/s and hurricane winds $U_{10} \sim 40$ m/s, suggests that stationary waves can be compared to Chen's for wave ages $c_p/ U_{10} < 0.25$ and (2) wave forms are comparable as to produce similar flow behavior. Square cleats on the rough belt were assumed to be 5 m high in full scale (length scale of 1:200) and most closely resemble WT3, where the vertical face is located on the upwind side. Here, length scales 1:100 and 1:150 produced full scale wave heights of 4 and 6 m. Mean C_D values matched those found by Chen (2007) with reasonably small standard deviations (Table 7). An important implication of this result is that as wind speed increases relative to the wave celerity ($c_p/U_{10} << 1$), waves can be taken to be 'stationary'.

Table 7: Mean total drag coefficient and standard deviation σ (computed from crest and trough values) for this experiment and Chen (2007). Column headings 1:100 and 1:150 refer to the length scales of simulation (full scale wave heights of 4 and 6 m) to bracket Chen's 5 m belt ('wave') heights for $c_p/U_{10} < 0.25$.

Parameter	Chen (2007)	1:100	1:150
$C_D \times 10^3$	9.83	9.08	11.2
$\sigma \times 10^3$	1.4	0.16	0.18

References

Anctil, F., and M. A. Donelan, 1996: Air–water momentum flux observations over shoaling waves. *J. Phys. Oceanogr.*, **26,** 1344–1353.

Chen, D., 2007: *Effects of moving waves on wind profile and wind stress - A wind tunnel study*. Ph.D. thesis, Texas Tech University, Lubbock.

Cook, N. J., 1977: Determination of the model scale factor in wind-tunnel simulations of the adiabatic atmospheric boundary layer. *J. Ind. Aero.*, **2**, 311–321.

Csanady, G. T., 1985: Air-sea momentum transfer by means of short-crested wavelets. *J. Phys. Oceanogr.*, **15**, 1486–1501.

Donelan, M.A., B. K. Haus, N. Reul, W. J. Plant, M. Stianssnie, H. C. Graber, O. B. Brown and E. S. Saltzman, 2004: On the limiting aerodynamic roughness of the ocean in very strong winds. *Geophys. Res. Lett.*, **31,** L18306.

Deardorff, J.W., 1967: Aerodynamic theory of wave growth with constant wave steepness. *J. Oceanographical Soc. Japan*, **41**, 453–480.

Gong, W., P. A. Taylor, and A. Dornbrack, 1999: Turbulent boundary-layer flow over fixed aerodynamically rough two-dimensional sinusoid waves. *J. Fluid Mech.*, **312**, 1–37.

Kawamura, H. and Y. Toba, 1988: Ordered motion in the turbulent boundary layer over wind waves. *J. Fluid Mech.*, **197**, 105–138.

Powell, M. D., P. J. Vickery, and T. A. Reinhold, 2003: Reduced drag coefficient for high wind speeds in tropical cyclones. *Nature*, **422**, 279-283.